Journal Name

ARTICLE

Low Temperature Synthesis Study of Metal-Organic Framework CPO-27: Investigating Metal, Solvent and Base Effects down to -78 °C

Received 00th January 20xx,
Accepted 00th January 20xx

DOI: 10.1039/x0xx00000x

www.rsc.org/

Simon M. Vornholt‡,[a] Susan E. Henkelis‡*[a] and Russell E. Morris[a]

CPO-27-M (M = Co, Mg, Ni, Zn) metal-organic frameworks have been successfully synthesized at temperatures down to -78 °C in a range of solvent systems and their crystallinity and morphology analyzed by powder X-ray diffraction and scanning electron microscopy. Mg- and Zn-CPO-27 could be synthesized at lower temperatures using MeOH-NaOH as the solvent with CPO-27-Zn showing the most crystalline material at -78 °C. CPO-27-Zn afforded the most crystalline samples of all studies in MeOH-TEA. However, in MeOH a non-porous monomeric [$Zn(H_2dhtp)(H_2O)_2$] complex was formed when no base was present. In THF with base (NaOH, TEA) the reaction produced crystalline MOFs in a controlled and stable manner at low temperatures, whilst the reagents were insoluble in THF at low temperature when no base was present. SEM was used to analyze the morphologies of the products.

Introduction

Metal-organic Frameworks, a rather recent field of study within material science, are porous two- or three-dimensional solids. These frameworks consist of a rigid organic linker that can coordinate to a secondary building unit (SBU) given by the metal coordination sphere of the metal salt.[1] The porosity of such MOFs can be tailored by altering the size of the linker and changing the metal salt with to which the linker coordinates.[2]
MOFs can achieve very high porosity giving them the potential for applications such as catalysis,[3] biomedicine,[4–8] gas adsorption and delivery,[4,9–14] and sensing.[15] Such MOFs are generally characterised by their extremely large Brunauer-Emmett-Teller surface areas (S_{BET}) approaching 10,000 $m^2 g^{-1}$ [16] and high structural/compositional flexibility.[15]
CPO-27-M (Coordination Polymer of Oslo) where M = Co,[17] Mg,[17–21] Ni,[2,12,17,21] Zn [9,15], (alternatively called M-MOF-74), is one of the world's most studied MOFs due to its large number of uncoordinated metal sites and exceptional potential for gas storage and separation.[15] Typically CPO-27 is produced under solvothermal conditions using high pressure and temperature.[13] However, recent developments have been made to the synthesis to reduce the temperature and scale up the reaction in aqueous conditions.[2,9,15]
Here we present an investigation on the effect of the metal cation, pH and solvent on the formation of CPO-27-Co, -Mg, -Ni and -Zn at reaction temperatures from 78 °C to -78 °C. This synthesis is, to the best of our knowledge, the first low temperature (below 0 °C) study to be performed on these MOFs. In the first part of this study, CPO-27-M (M = Co, Mg, Ni, Zn) was formed in methanol as solvent with 1M sodium hydroxide as base. Since the afforded samples for CPO-27-Zn showed crystalline materials at each temperature, different combinations of solvent and base (MeOH-TEA **(2)**, MeOH-no base **(3)**, THF-no base **(4)**, THF-NaOH **(5)**, THF-TEA **(6)**) were also tried. All solids were characterised by powder X-ray diffraction (PXRD) and the materials made at the lowest temperature were investigated using scanning electron microscopy (SEM). The results presented within this paper are the first CPO-27-M metal-organic frameworks to have been successfully synthesized at -78 °C.

Experimental

Materials and methods

All reagents and solvents were obtained from commercial sources and were used without further purification.

CPO-27-M typical synthesis: Zinc acetate dihydrate (1.11 g, 5.00 mmol) was dissolved in methanol (12.3 mL, 304 mmol) with vigorous stirring at 0 °C (referred to as Solution A). 2,5-dihydroxyterephthalic acid (0.50 g, 2.50 mmol) was dissolved in sodium hydroxide (1 M, 10.0 mL, 10.0 mmol) and cooled to 0 °C (referred to as Solution B). Solution B was then added dropwise over a period of 5 minutes and the resulting mixture allowed to stir for 6 h, with a sample taken after 3 h. The precipitate was collected via filtration, washed with water (3 x 100 mL) and allowed to dry in air overnight to yield a yellow solid.

[a] School of Chemistry, Purdie Building, North Haugh, St Andrews, Fife, KY16 9ST, UK
† ‡ These authors contributed equally. * Corresponding author.
Electronic Supplementary Information (ESI) available: [PXRD patterns for all temperatures and samples, Pawley refinement of monomeric [$Zn(H_2dhtp)(H_2O)_2$], and SEM images]. See DOI: 10.1039/x0xx00000x

Table 1. Composition of solutions A and B, reaction temperatures and percentage yields for all CPO-27-M afforded.

Sample	Composition of Solution A		Solution B	Temperature / [°C]	Yield* / [%]
	Metal Salt / [g]	Solvent /[mL]	Base / [mL]		
CPO-27-Co(*1*)	$Co(OAc)_2•4H_2O$, 1.25	MeOH, 17.7	1 M NaOH, 10	78, 25, 0	80.14, 70.96, 69.82
CPO-27-Mg(*1*)	$Mg(NO_3)_2•6H_2O$, 1.28	MeOH, 17.7	1 M NaOH, 10	78, 25, 0, -20	59.31, 48.05, 47.30, 27.15
CPO-27-Ni(*1*)	$Ni(OAc)_2•4H_2O$, 1.24	MeOH, 17.7	1 M NaOH, 10	78, 25, 0	85.84, 70.38, 72.33
CPO-27-Zn(*1*)	$Zn(OAc)_2•2H_2O$, 1.11	MeOH, 17.7	1 M NaOH, 10	78, 25, 0, -20, -40, -78	60.35, 58.13, 42.37, 38.81, 38.57, 15.36
CPO-27-Zn(*2*)	$Zn(OAc)_2•2H_2O$, 1.11	MeOH, 17.7	TEA+H_2O, 2.15+2	78, 25, 0, -20, -40, -78	62.25, 60.19, 56.47, 20.51, 16.24, 35.80
CPO-27-Zn(*3*)	$Zn(OAc)_2•2H_2O$, 1.11	MeOH, 17.7	H_2O, 10	78, 25, 0	75.29, 72.06, 72.46
CPO-27-Zn(*4*)	$Zn(OAc)_2•2H_2O$, 1.11	THF, 12.3	H_2O, 10	78, 25, 0	69.69, 25.90, 19.56
CPO-27-Zn(*5*)	$Zn(OAc)_2•2H_2O$, 1.11	THF, 12.3	1 M NaOH, 10	78, 25, 0, -20, -40, -78	44.83, 44.91, 46.65, 22.57, 31.84, 18.22
CPO-27-Zn(*6*)	$Zn(OAc)_2•2H_2O$, 1.11	THF, 12.3	TEA+H_2O, 2.15+2	78, 25, 0, -20, -40	32.63, 49.58, 66.67, 48.47, 19.88

Characterization Techniques

Powder X-ray diffraction data (PXRD) were collected on a Panalytical Empyrean diffractometer operating Cu Kα1 radiation monochromated with a curved Ge(111) crystal in reflectance mode. Samples taken halfway through the reaction were loaded into capillaries and analysed on a STOE STADIP diffractometer operating Cu Kα1 radiation. Powder X-ray patterns have been compared with an X-ray powder pattern of CPO-27-Zn, derived from single crystal data. [22]

SEM imaging was carried out on a FEI Scios Dualbeam, with a resolution of 1 nm and a voltage of 2000 V to 30 kV. For the imaging, the SEM was operated between 1 - 5 kV at 10 - 50 pA. The unground sample, as synthesized, was placed on a carbon tab prepared, aluminium stub disc. Furthermore, the samples were brushed with Ag-paste and Au-sputter-coated (15 mA/30 sec).

Nitrogen sorption measurements were carried out on a micrometrics TriStar II. Samples have been degassed at a FlowPrep™ 060 for 12h at 150 °C. Results have been analysed using the Rouquerol[23] method.

Nitric oxide (NO) release profiles were measured using a Sievers NOA 280i chemiluminescence nitric oxide analyser.

Results and discussion

Each CPO-27-M synthesis was carried out in a molar ratio of 2.5:5:10:304 for linker:metal-salt:base:solvent. This is a modified version of a given ratio that has been proven successful for the formation of each MOF by Maspoch and co-workers.[15] As the samples were left to dry in air overnight and characterized as-synthesized, we assume a molecular formula of $[M_2(C_8H_2O_6)(H_2O)_2] \cdot 8H_2O$ (M = Co, Mg, Ni, Zn). For the first part of this study methanol as solvent and aqueous 1M sodium hydroxide were used. The acetate salt was used for Co, Ni and Zn and the nitrate salt for Mg. Under these basic conditions the linker solution is assumed to be fully deprotonated and visual inspection shows the salt to be fully dissolved in the organic solvent. For syntheses at temperatures lower than 0 °C a solvent/dry ice bath was employed. Methanol and water were used as solvent for reactions at -20 °C and -40 °C, with acetone used for all reactions considered at -78 °C. All reactions were carried out for 6h and a sample was taken halfway through the procedure to check the progress of crystallization.

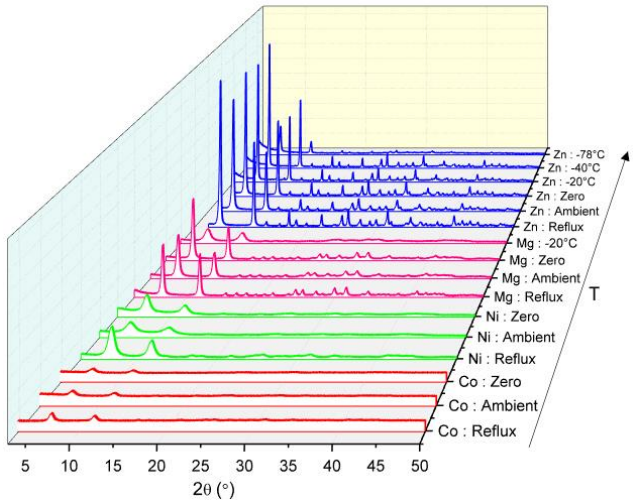

Fig. 1 Comparison of the powder X-ray diffraction patterns for CPO-27-Co(1), -Ni(1), -Mg(1) and –Zn(1) from a MeOH-NaOH solution with changing temperature. Co – red; Ni – green; Mg – pink; Zn – blue.

The Effect of the Metal Cation

As Figure **1** depicts, CPO-27-Zn exhibits high crystallinity throughout all temperatures. The two main peaks at 6.8° and 11.7° 2θ, which are characteristic for the CPO-27-M family, are clearly visible and show high intensity down to -78 °C. The fingerprint region can be seen clearly down to -40 °C. Apart from the latter mentioned, have all materials phase purity, the material obtained at -40 °C shows two additional non-CPO-27 peaks at 9.6 ° and 10.9 ° 2θ of low intensity. However, the sample synthesized at -78 °C, shows less intensity in comparison to those samples synthesized at higher temperatures. Therefore, we assume that the framework has not fully formed under those conditions, consistent with the reduced rate of reaction at lower temperatures.

The magnesium analogue shows an interesting sensitive behaviour regarding the solvent and deprotonation of the acidic proton on the H_4dhtp. We report the successful synthesis of porous CPO-27-Mg down to temperatures of 0 °C. When the formation temperature was further reduced to -20 °C, the characteristic CPO-27 peaks can be seen, although visibly broadened, whilst the fingerprint area is no longer distinct. This can be seen clearly from Figure **1**, with crystalline samples produced preferentially at higher temperatures. Mg^{2+} is a relatively hard, hydrophilic cation, and with methanol as the lone solvent pure CPO-27-Mg was able to be successfully produced down to -20 °C.

The XRD patterns for CPO-27-M (M = Co, Ni) show a large signal:noise ratio for all temperatures. However, it can be stated that the framework has still been formed, at least in part, as the characteristic CPO-27 peaks are clearly seen.

The Effect of Methanol as Solvent

From these results, further experiments were undertaken with zinc acetate under varying solvent and pH-conditions. Figure **2** shows the XRD patterns of the samples synthesized in methanol as solvent with triethylamine (TEA) as base. This solvent – base system shows remarkably sustained crystallinity down to temperatures of -78 °C. After addition of the basic linker solution to the salt solution, the rather bulky triethylammonium-ion shields access to the Zn^{2+}-ions and therefore leads to a more controlled manner of formation and crystallization.

A sample was collected after 3h and at -78 °C we can already see the formation of the characteristic CPO-27-framework. However, samples synthesized at temperatures of -40 °C and lower show a slight shift of 0.2 2θ of each peak in the XRD patterns. This can be explained by a shrinkage in unit cell dimensions at lower temperatures. However, a comparison with phase-pure CPO-27-Zn, confirms that there is no other phase present in any of the materials obtained from this solvent-base system.

In 2007, Ghermani reported a three-dimensional, non-porous species $[Zn(H_2dhtp)(H_2O)_2]$ that could be obtained when the linker is not fully deprotonated.[24] In this study, we confirmed these findings by conducting the reaction in a methanol-water solvent mixture at pH 7. The addition of the linker to the translucent salt solution produces an off-white suspension within minutes. Although this process is slowed down at lower temperatures, the same, highly crystalline product is obtained

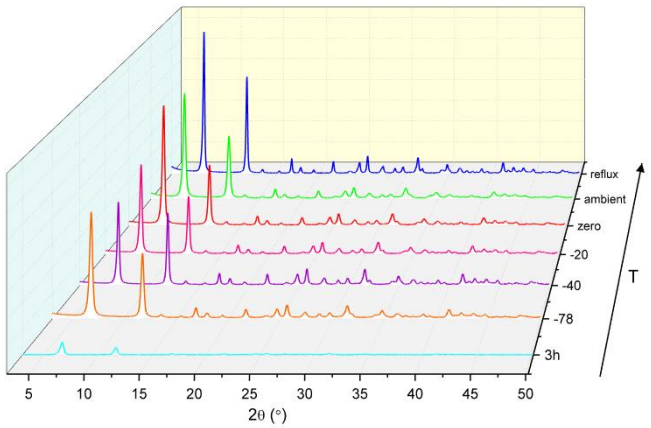

Fig. 2 Powder X-ray diffraction patterns for CPO-27–Zn(2) afforded from a MeOH-TEA solution with temperature ranging from -78 °C to reflux. A sample was taken half way through each synthesis at the 3 hour mark and analysed, the 3h sample for -78°C is presented here. Reflux – blue; ambient – green; 0 °C – red; -20 °C – pink; -40 °C – purple; -78 °C – orange; -78 °C_3h – cyan.

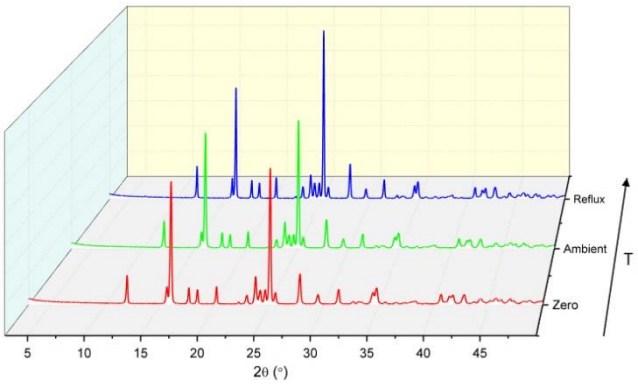

Fig. 3 Powder X-ray diffraction patterns for a Zn(II) complex of 2,5-dihydroxyterephthalic acid afforded from a CPO-27–Zn(3) synthesis attempt in methanolic solution without base.22 Reflux – blue; ambient – red; 0 °C – green.

by the synthesis at temperatures down to 0 °C, without structural changes in the unit cell parameters (Figure **3**). A Pawley refinement using the Topas program suite [25] for $[Zn(H_2dhtp)(H_2O)_2]$ was carried out against in-house X-ray diffraction data, using a model structure produced by Ghermani (See Figure S11 in Supplementary).[24] This non-porous structure is very similar to a Mg-H_2dhtp complex with composition $Mg(H_2dhtp)(H_2O)_5{\cdot}H_2O$ that we produced in 2016 through a lowering of the amount of NaOH in reaction conditions normally used to produce CPO-27-Mg by the reflux method.[25]

The Effect of Tetrahydrofuran as Solvent

Interestingly, a different behaviour is observed if the solvent is changed to aqueous THF. For that reaction set, the zinc acetate salt was dissolved in THF and left stirring until it reached the desired temperature. An aqueous solution of the linker was then added to the salt solution over a period of 5 minutes.
Similarly, to methanol, when the aqueous linker solution is added to a stirred solution of the metal salt in THF a milky-yellow suspension is produced after 5 minutes. This effect is, once again slowed down at lower temperatures. However, a

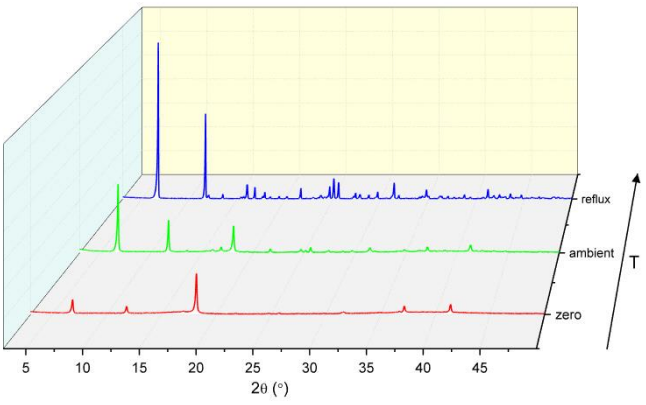

Fig. 4 Powder X-ray diffraction patterns for CPO-27–Zn(4) afforded from a THF solution without base. Products decrease in crystallinity and purity as the temperature is decreased towards 0 °C. Reflux – blue; ambient – green; 0 °C – red.

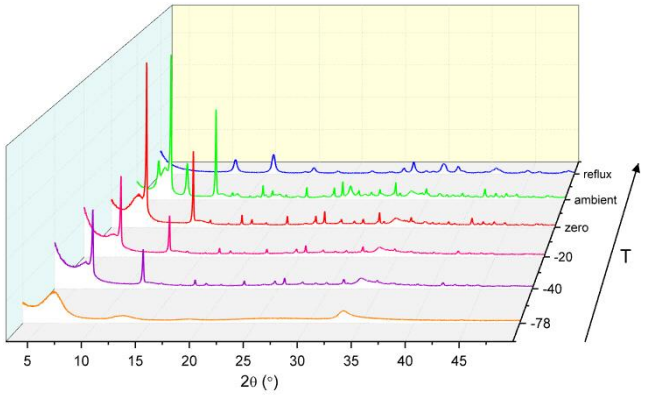

Fig. 5 Powder X-ray diffraction patterns for CPO-27-Zn(5) afforded from a THF-NaOH solution with a temperature range from reflux to -78 °C. Reflux – blue; ambient – green; 0 °C – red; -20 °C – pink; -40 °C – purple; -78 °C – orange.

comparison with pure CPO-27-Zn indicates another phase in the diffraction pattern for reactions carried out at both reflux and ambient conditions (Figure **4**). This phase could be identified as monomeric species. The product synthesized at 0 °C began to lose crystallinity when in comparison to higher temperatures, but the pattern shows now just the characteristic low angle and fingerprint peaks of CPO-27-Zn. The partial solubility of the H_4dhtp linker in THF explains these results. During the addition of the linker suspension, the linker gradually dissolves in the THF:H_2O solvent mixture, while the dissociated acetate-ion of the zinc salt can slowly, and in a controlled manner, deprotonate the linker. However, the reduction of temperature has a substantial impact on the solubility of each reagent. Therefore, we assume that a further reduction of the reaction-temperature will lead to pure CPO-27-Zn but also continue to reduce the solubility and slow down the rate of formation.
Comparable to when methanol was used as solvent, both NaOH and TEA were used as base with THF, this produced a more controlled formation of the CPO-27 framework at lower temperatures. With NaOH (Figure **5**), all patterns show a shoulder at 6° 2θ and another broad peak in the fingerprint area at 33° 2θ. The shoulder on the first main peak gradually loses intensity, as the reaction temperature gets colder. Interestingly, a sample taken after 3h for the reaction at -40 °C shows neither the shoulder nor the high angle peak, while characteristic parts of the framework are already formed (see supplementary information), this suggests that a shorter reaction time of 3h may be suitable for this solvent system.
As the linker is already deprotonated before mixing with the salt solution, we can determine that at warmer temperatures, the deprotonated linker is reactive enough for competing reaction pathways. Cooling the reaction down, slows down the kinetics of the molecules in solution, allowing for a more controlled formation of the MOF.
Similar findings can be found for the reaction system THF:TEA, with crystalline samples produced at lower temperatures (Figure **6**). The desired framework can be afforded by decreasing the temperature to ambient conditions, once again

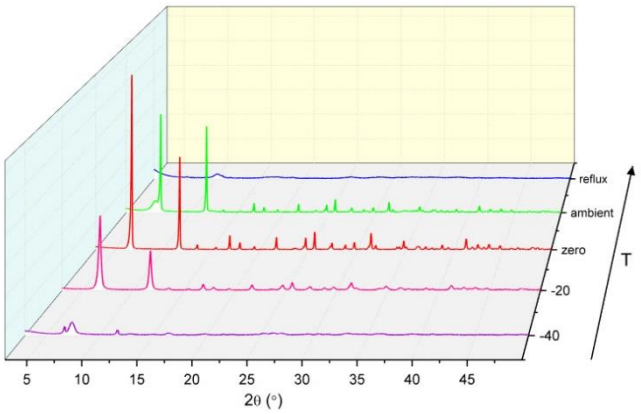

Fig. 6. Powder X-ray diffraction patterns for CPO-27–Zn(6) afforded from a THF-TEA solution with changing temperature. Only products afforded from reactions conducted at zero and -20 °C yielded pure results. Reflux – red; ambient – orange; 0 °C – yellow;

a shoulder at 6 °2θ can be seen indicating a change in the size and shape of the unit cell of the MOF. Further reduction of the temperature to -20 °C yields CPO-27-Zn materials without changes in the unit cell, in a controlled manner. When the synthesis was conducted at -40 °C the material loses crystallinity and the characteristic low angle peaks almost disappear. Again, fully formed crystalline MOF samples can be seen after 3 hours at all temperatures except reflux, as such showing that the reaction time in THF is too long after 6 hours.

SEM studies were conducted on each of the materials, obtained from the lowest successful reaction temperature. Each sample was taken as synthesized and prepared for investigation without further grinding. Images were taken at scales of 1 mm, 100 µm and 10 µm to investigate the potentially different morphologies. Figure **7** displays selected SEM images for the reaction system MeOH:H_2O:NaOH for cobalt and zinc (all materials will be discussed, see supplementary information for full SEM analysis). All materials show large agglomerates of a few hundred µm size, with sharp edges, at 10 µm. At 100 µm the CPO-27-M (M = Ni, Co) remain as large agglomerates and plates with sharp edges, whereas the zinc and magnesium analogous already show a more powdery, softer morphology. At 1 mm, all materials show small conglomerates with a "cotton- ball" morphology.

From the SEM analysis of the remaining zinc samples in different solvent systems, it became clear that the solvent makes a large impact on the morphology of the desired MOF (Figure **8**). Solids produced from all methanolic solvents yield "cotton-ball" like morphologies with the monomeric species yielding very fine powder and at higher scale, agglomerates built up from plates.

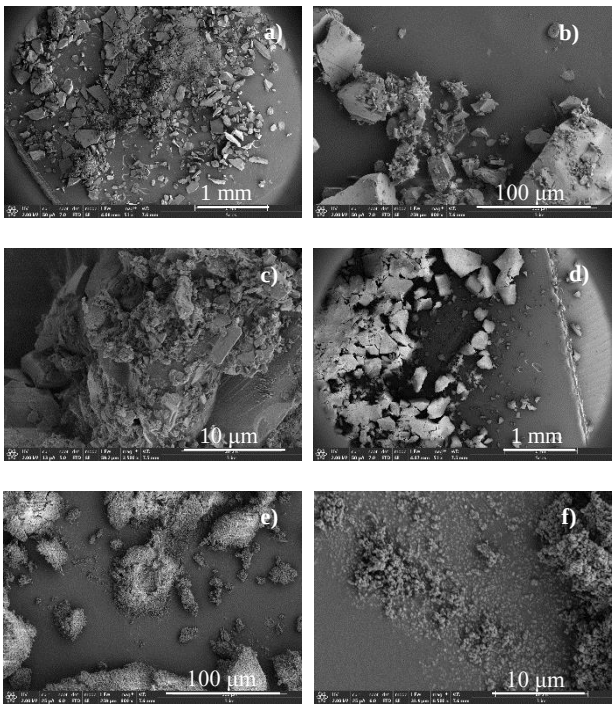

Fig. 7 SEM images a - c for CPO-27-Co**(1)** afforded from a MeOH-NaOH solution at a reaction temperature of 0 °C; SEM images d – f show CPO-27-Zn**(1)** afforded from a MeOH-NaOH solution at -78 °C.

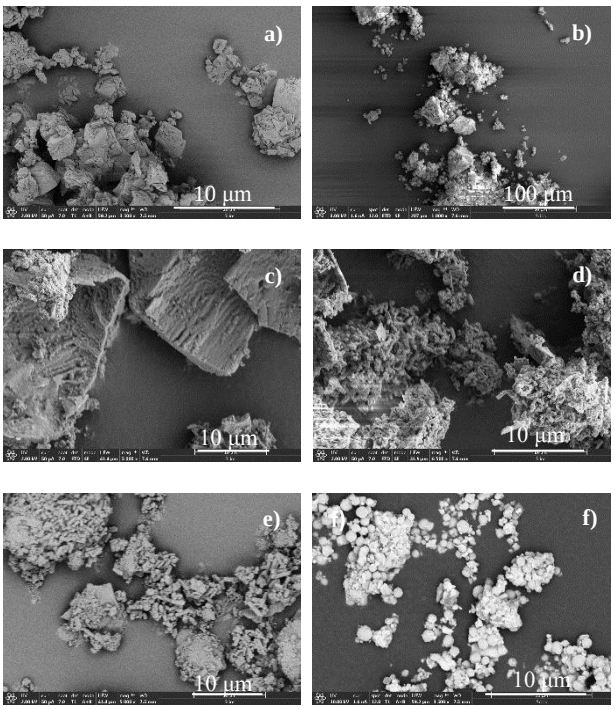

Fig. 8 SEM images for CPO-27-Zn afforded from: a – MeOH-H_2O solution without base at ambient **(3)**; b – MeOH-TEA solution at -78 °C **(2)**; c and d – THF-NaOH solution at -40 °C **(5)**; e – THF-TEA solution at -78 °C **(6)**; f – THF-H_2O solution without base at ambient **(4)**.

However, when the solvent is changed to THF, the morphology of the MOF changes. For THF with base (NaOH, TEA) low scale images show powdery agglomerates without sharp edges. Flake-like agglomerates, built up from rods are seen at 100 µm. Images at increased scale show these rods more clearly. Interestingly, the cotton-ball like morphology is once again seen for the sample obtained from an aqueous THF solution without base. Therefore, we can conclude that protic solvents, such as methanol, yields ball-like morphologies. Contrary to this, when an aprotic solvent, tetrahydrofuran, is used with a base the morphology changes and elongates into rods.

Selected materials have been taken for nitrogen sorption studies. Due to the given parameters and set up of the device, the full micropore-volume might not have been accessed. However, we could conclude the trend, that CPO-27-Zn materials have a higher BET surface area than the other metal analogues CPO-27-M (M=Co, Ni, Mg) and that the BET surface area decreases with decreasing reaction temperatures. As recently reported by Cattaneo et al. [9] does a small BET surface area not necessarily correlate with a low uptake and storage of other guest molecules or gases. Additionally, point Rouquerol et al. out that the BET equation is not ideal for microporous adsorbents. [23] Therefore, CPO-27-Zn (**2**), obtained from reflux, 0 °C and -78°C, as well as CPO-27-Ni (**1**), obtained from reflux, have been analysed regarding their nitric oxide (NO) uptake and release. All of these four tested materials, show a significant NO release profile (in the µmol NO per gram material), within the range of biological activity over 10h.[9]

Conclusions

Here we have shown that the metal source has a large effect on whether the material can form at low temperatures. It is clear that non-transition metals (Mg, Zn) are easier to form than such transition metals (Co, Ni). CPO-27-Zn showed the most promising material throughout the temperature range and produced a pure crystalline material in MeOH-NaOH. This was therefore taken forward as the most likely candidate to produce crystalline solids in different solvent systems. CPO-27-Zn proved successful in methanol and formed down to temperatures of -78 °C. However, in MeOH, the reaction formed a non-porous monomeric [Zn(H_2dhtp)(H_2O)$_2$] when no base was present. Reactions conducted in THF proved difficult, the reactions proceeded without concern at warm temperatures, with only colder temperatures forming the MOF in a controlled manner, whilst the reagents are insoluble without base in cold temperatures.

Acknowledgements

We thank Sylvia Williamson and Maria Nowosielska for their support with the BET measurements, the EPSRC (EP/K005499/1) (EP/K503162/1) for their financial support of this project and the EPSRC Capital for Great Technologies (EP/L017008/1).

References

(1) Wang, L. J.; Deng, H.; Furukawa, H.; Gándara, F.; Cordova, K. E.; Peri, D.; Yaghi, O. M.; Gimeno-Fabra, M.; Munn, A. S.; Stevens, L. a.; Drage, T. C.; Grant, D. M.; Kashtiban, R. J.; Sloan, J.; Lester, E.; Walton, R. I.; Wang, L. J.; Deng, H.; Furukawa, H.; Gándara, F.; Cordova, K. E.; Peri, D.; Yaghi, O. M. *Inorg. Chem.* **2014**, *48* (12), 5881–5883.

(2) Guasch, J.; Dietzel, P. D. C.; Collier, P.; Acerbi, N. *Microporous Mesoporous Mater.* **2015**, *203*, 238–244.

(3) Ruano, D.; Díaz-García, M.; Alfayate, A.; Sánchez-Sánchez, M. *ChemCatChem* **2015**, *7* (4), 674–681.

(4) Allan, P. K.; Wheatley, P. S.; Aldous, D.; Mohideen, M. I.; Tang, C.; Hriljac, J. A.; Megson, I. L.; Chapman, K. W.; De Weireld, G.; Vaesen, S.; Morris, R. E. *Dalt. Trans.* **2012**, *41* (14), 4060.

(5) Hinks, N. J.; McKinlay, A. C.; Xiao, B.; Wheatley, P. S.; Morris, R. E. *Microporous Mesoporous Mater.* **2010**, *129* (3), 330–334.

(6) McKinlay, A. C.; Allan, P. K.; Renouf, C. L.; Duncan, M. J.; Wheatley, P. S.; Warrender, S. J.; Dawson, D.; Ashbrook, S. E.; Gil, B.; Marszalek, B.; Düren, T.; Williams, J. J.; Charrier, C.; Mercer, D. K.; Teat, S. J.; Morris, R. E. *APL Mater.* **2014**, *2* (12), 124108.

(7) Miller, S. R.; Alvarez, E.; Fradcourt, L.; Devic, T.; Wuttke, S.; Wheatley, P. S.; Steunou, N.; Bonhomme, C.; Gervais, C.; Laurencin, D.; Morris, R. E.; Vimont, A.; Daturi, M.; Horcajada, P.; Serre, C. *Chem. Commun. (Camb).* **2013**, *49* (71), 7773–7775.

(8) Rojas, S.; Wheatley, P. S.; Quartapelle-Procopio, E.; Gil, B.; Marszalek, B.; Morris, R. E.; Barea, E. *CrystEngComm* **2013**, *15* (45), 9364.

(9) Cattaneo, D.; Warrender, S. J.; Duncan, M. J.; Castledine, R.; Parkinson, N.; Haley, I.; Morris, R. E. *Dalton Trans.* **2015**, *45* (2), 618–629.

(10) Chavan, S.; Bonino, F.; Valenzano, L.; Civalleri, B.; Lamberti, C.; Acerbi, N.; Cavka, J. H.; Leistner, M.; Bordiga, S. *J. Phys. Chem. C* **2013**, *117* (30), 15615–15622.

(11) Chavan, S.; Vitillo, J. G.; Groppo, E.; Bonino, F.; Lamberti, C.; Dietzel, P. D. C.; Bordiga, S. *J. Phys. Chem. C* **2009**, *113* (8), 3292–3299.

(12) Dietzel, P. D. C.; Panella, B.; Hirscher, M.; Blom, R.; Fjellvåg, H. *Chem. Commun.* **2006**, No. 9, 959.

(13) Grant Glover, T.; Peterson, G. W.; Schindler, B. J.; Britt, D.; Yaghi, O. *Chem. Eng. Sci.* **2011**, *66* (2), 163–170.

(14) McKinlay, A. C.; Eubank, J. F.; Wuttke, S.; Xiao, B.; Wheatley, P. S.; Bazin, P.; Lavalley, J.-C.; Daturi, M.; Vimont, A.; De Weireld, G.; Horcajada, P.; Serre, C.; Morris, R. E. *Chem. Mater.* **2013**, *25* (9), 1592–1599.

(15) Garzón-Tovar, L.; Carné-Sánchez, A.; Carbonell, C.; Imaz, I.; Maspoch, D. *J. Mater. Chem. A* **2015**, *3* (41), 20819–20826.

(16) Furukawa, H.; Cordova, K. E.; O'Keeffe, M.; Yaghi, O. M.; O'Keeffe, M.; Yaghi, O. M. *Science (80-.).* **2013**, *341* (6149), 1230444.

(17) Dietzel, P. D. C.; Georgiev, P. A.; Eckert, J.; Blom, R.; Strässle, T.; Unruh, T. *Chem. Commun. (Camb).* **2010**, *46* (27), 4962–4964.

(18) Yang, D.-A.; Cho, H.-Y.; Kim, J.; Yang, S.-T.; Ahn, W.-S. *Energy Environ. Sci.* **2012**, *5* (4), 6465–6473.
(19) McKinlay, A. C.; Xiao, B.; Wragg, D. S.; Wheatley, P. S.; Megson, I. L.; Morris, R. E. *J. Am. Chem. Soc.* **2008**, *130* (31), 10440–10444.
(20) Kahr, J.; Morris, R. E.; Wright, P. A. *CrystEngComm* **2013**, *15* (45), 9779.
(21) Magdysyuk, O. V; Adams, F.; Liermann, H.-P.; Spanopoulos, I.; Trikalitis, P. N.; Hirscher, M.; Morris, R. E.; Duncan, M. J.; McCormick, L. J.; Dinnebier, R. E. *Phys. Chem. Chem. Phys.* **2014**, *16* (43), 23908–23914.
(22) Dietzel, P. D. C.; Johnsen, R. E.; Blom, R.; Fjellvåg, H. *Chem. - A Eur. J.* **2008**, *14* (8), 2389–2397.
(23) Rouquerol, J.; Llewellyn, P.; Rouquerol, F. *Stud. Surf. Sci. Catal. 160*, 49–56.
(24) Ghermani, N. E.; Morgant, G.; d'Angelo, J.; Desmaële, D.; Fraisse, B.; Bonhomme, F.; Dichi, E.; Sgahier, M. *Polyhedron* **2007**, *26* (12), 2880–2884.
(25) Henkelis, S. E.; McCormick, L. J.; Cordes, D. B.; Slawin, A. M. Z.; Morris, R. E. *Inorg. Chem. Commun.* **2016**.